Acta Oceanol. Sin., 2018, Vol. 37, No. 7, P. 41–54
DOI: 10.1007/s13131-018-1205-5
http://www.hyxb.org.cn
E-mail: hyxbe@263.net

Rare earth elements and yttrium in ferromanganese deposits from the South China Sea: distribution, composition and resource considerations

ZHONG Yi[1, 2, 3], CHEN Zhong[1]*, GONZALEZ Francisco Javier[4], ZHENG Xufeng[1], LI Gang[1], LUO Yun[1, 3], MO Aibin[1, 3], XU Antao[1, 3], WANG Shuhong[1]

[1] Key Laboratory of Ocean and Marginal Sea Geology, South China Sea Institute of Oceanology, Chinese Academy of Sciences, Guangzhou 510301, China

[2] Department of Marine Science and Engineering, Southern University of Science and Technology of China, Shenzhen 518055, China

[3] University of Chinese Academy of Sciences, Beijing 100049, China

[4] Geological Survey of Spain (IGME), Madrid 28003, Spain

Received 14 June 2017; accepted 10 October 2017

Abstract

Ferromanganese nodules and crusts contain relatively high concentration of rare earth elements (REE) and yttrium (REY), with a growing interest in exploitation as an alternative to land-based REY resources. On the basis of comprehensive geochemical approach, the abundance and distribution of REY in the ferromanganese nodules from the South China Sea are analyzed. The results indicate that the REY contents in ferromanganese deposits show a clear geographic regularity. Total REY contents range from 69.1×10^{-6} to $2\,919.4\times10^{-6}$, with an average value of $1\,459.5\times10^{-6}$. Especially, the enrichment rate of Ce content is high, accounting for almost 60% of the total REY. This REE enrichment is controlled mainly by the sorption of ferromanganese oxides and clay minerals in the nodules and crusts. Moreover, the total REY are higher in ferromanganese deposits of hydrogenous origin than of diagenetic origin. Finally, Light REE (LREE) and heavy REE (HREE) oxides of the ferromanganese deposits in the study area can be classified into four grades: non-enriched type, weakly enriched type, enriched type, and extremely enriched type. According to the classification criteria of rare earth resources, the Xisha and Zhongsha platform-central deep basin areas show a great potential for these rare earth metals.

Key words: ferromanganese deposits, rare earth elements and yttrium, abundance characteristics, controlling factors, potential source, South China Sea

Citation: Zhong Yi, Chen Zhong, Gonzalez Francisco Javier, Zheng Xufeng, Li Gang, Luo Yun, Mo Aibin, Xu Antao, Wang Shuhong. 2018. Rare earth elements and yttrium in ferromanganese deposits from the South China Sea: distribution, composition and resource considerations. Acta Oceanologica Sinica, 37(7): 41–54, doi: 10.1007/s13131-018-1205-5

1 Introduction

The rare earth elements (REE) are a group of 15 "lanthanide" elements from lanthanum to lutetium on the periodic table, as well as yttrium, which is usually comprised because of similar chemical properties (Long et al., 2012). Over recent decades, rare earth elements and yttrium (REY) play essential roles in a variety of highly advanced devices and green technologies such as defence metallurgy, consumer electronics, medical applications, etc (Kynicky et al., 2012; Van Gosen et al., 2014). The world's most commercially important REE deposits are found in alkaline igneous rocks and carbonatites (Orris and Grauch, 2002). The estimated total world reserve of rare earth oxides on land is about 114 Mt, 48% of which is in China (Kynicky et al., 2012), such as Bayan Obo Mining District in northern China (Chi et al., 2012; Su, 2009). As a result, global rare metals consumption has been steadily increased, but supplies have not always been reliable due to the limited number of leading manufacturers. Increased competition for metal resources from rapidly expanding economies, such as China, India, Brazil and Indonesia, may lead to a shortage in the future (Hein et al., 2013). Demand for the REE is expected to grow by at least 6% per year over the next 25 a, particularly for permanent magnets and medical technologies (Alonso et al., 2012), and this, coupled with China's increased internal demand (Weng et al., 2015), has led to concern about the risk of supply shortage. Therefore, to maintain a stable supply of REEs to industry, it is important to ensure there are a variety of REE resources.

Recently, Kato et al. (2011) have discovered a new type of mineral resource, named REY-rich mud, distributed in vast quantities throughout a large part of the Pacific Ocean. There is no doubt that the index of progress in the exploration, exploitation, beneficiation technologies as well as mining technology concerning deep sea mineral resources, proved that in addition to the REY-rich deep sea mud, there is also a distinct REE type of mineralization associated with deep sea ferromanganese crusts and polymetallic nodules (Papavasileiou, 2014). New REY mines

Foundation item: The National Natural Science Foundation of China under contract Nos 41376057, 41306047, 41676056; the Spanish project SUBVENT under contract No. CGL2012-39524-C02.
*Corresponding author, E-mail: chzhsouth@scsio.ac.cn

such as nodule/crust or deep see mud in deep sea have been paid a lot of attention for their high content of REY and enrichment of HREE recently. Ferromanganese crusts, also referred to as Co-rich crusts, are formed principally by hydrogenetic precipitation from the cold sea water of colloidal particles of Fe and Mn oxyhydroxides onto rock substrates (Dymond et al., 1984; Bau et al., 1996; Hein et al., 2000; Schulz, 2006). Hydrogenetic crusts concentrate REY at many orders of the magnitude above their concentration in sea water (Bau et al., 1996; Hein et al., 2013), which is promoted by the high reaction surface area of Fe-Mn oxyhydroxides (Hein et al., 2013; Pourret and Davranche, 2013), slow oxidation reaction kinetics, and slow growth rates (Bau and Dulski, 1996). Polymetallic nodules constitute mixed-source deposits formed by hydrogenetic and diagenetic precipitation of Fe-Mn colloids around a nucleus on the surface of soft sediments (Halbach et al., 1988). Interactions of both hydrogenetic and diagenetic processes lead to a range of bulk Mn/Fe ratios from 1.0 to 2.5 for oxic diagenesis and up to 50.0 when the sedimentary column is suboxic near the seabed (Calvert and Piper, 1984; Schulz, 2006). Metals (Ni, Cu and Co), REY in nodules are mainly derived from sea water through hydrogenetic precipitation and further enrichment in metallic elements (Mn, Cu, Ni and Zn) occurs via diagenetic precipitation (Ohta et al., 1999). This makes ferromanganese deposits a potential resource for many of the metals used in emerging high-technology and green-technology applications (Hein et al., 2013), thus, mapping the global distribution of REY-rich ferromanganese deposits has become an important issue.

Recent studies on REE geochemical characteristics of ferromanganese nodules and crusts have focused more on open-oceans from areas such as the prime crust zone in the equatorial Pacific, the central East Indian Basin, the Peru Basin and Penrhyn-Samoa Basins in the southeastern Pacific Ocean (Rona, 2008; Kuhn et al., 2012; Hein et al., 2013). Only a few studies have focused on continental margin ferromanganese nodules and crusts from Galicia Bank (NW Atlantic Iberia margin) (González et al., 2016), the Gulf of Cadiz (González et al., 2012), California continental-margin (Hein et al., 2005; Conrad et al., 2017), Canary Island Seamount Province (Marino et al., 2017) and the Philippine Sea (Xu et al., 2006).

As is one of the largest marginal seas in the western Pacific Ocean, the South China Sea (SCS) is subjected to relatively large terrigenous inputs, metal fluxes from continental shelf and slope hypoxic sediment, seasonal upwelling, high primary productivity, and a well-developed oxygen minimum zone (Liu and Colin, 2010; Milliman and Farnsworth, 2011). A large number of ferromanganese nodules have been found to be densely distributed on the Jiaolong Seamount in the deep-sea basin, where their source potential is more promising than ocean nodules (Zhang et al., 2015). Many researchers have pointed out that REY as a powerful tool for defining modern and past geological environments and helps to understand its source and distribution because of their unique behavior during various geochemical process (Wang et al., 1984; Bao and Li, 1993; Zhang et al., 2012). However, the systematic study of the potential REY mineral sources for the nodule/crust in the SCS, and the knowledge of their distribution and enrichment mechanism are uncertain.

This paper presents geochemical and mineralogical descriptions of ferromanganese nodule and crust samples recovered from the SCS from 2005 to 2013. Then, by combining the new data with previously constructed data set, we determine the spatial distribution and variations of REE in the ferromanganese nodules and crusts throughout the SCS. In addition, we also discuss the key controlling factors that lead to REE enrichment and its global significances.

2 Sampling and experiments

2.1 *Sampling*

As part of the integrated investigation cruises organized by the South China Sea Institute of Oceanology (SCSIO, Chinese Academy of Sciences), 16 ferromanganese nodule and crust samples have been collected from eight stations in the SCS since 2005 (Fig. 1 and Table 1). Five stations (05E105, 05E202, 05E204, 10E204B and ZX31) are located in the northeastern SCS, while two stations (05E107 and 09KJ22) are in the northwestern SCS. The Station J-158 is located in the central basin of the SCS and with the water depth of 3 573 m on the Jiaolong Seamount.

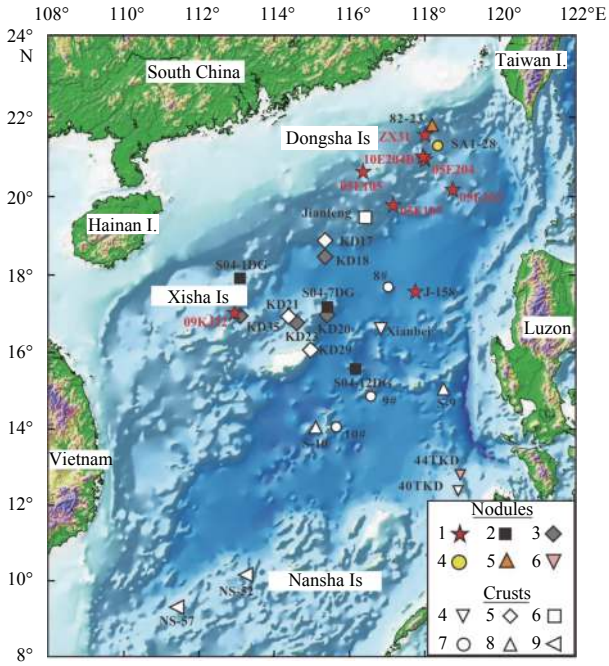

Fig. 1. Sampling location of ferromanganese nodules and crusts in the SCS. 1. This study, 2. from Zhang et al. (2012), 3. from Bao and Li (1993), 4. from Chen and Gui (1998), 5. from Bao and Li (1993), 6. from Liang et al. (1991), 7. from Yao et al. (1994), 8. from Wang et al. (1984), and 9. from Chen et al. (2006b).

2.2 *Mineralogical and geochemical analysis*

The X-ray powder diffraction (XRD) was conducted using a PANalytical X'Pert PRO diffractometer equipped with Cu-Kα radiation, carbon monochromator and automatic slit (PTRX-004). The analytical conditions for the XRD were: Cu-Kα radiation at 40 kV and 30 mA, a curved graphite secondary monochromator, scans from 2–70 (2θ), step size of 0.017 0 (2θ) and step time 0.5°/min. As the intensity of a mineral diffraction pattern in a mixture is proportional to its concentration, measuring a mineral peak areas provide an estimate for the relative mineral abundance in a sample.

For major, trace and REE analysis, 40 mg of dried and ground sample powders were weighed into a teflon beaker. After 0.5 mL HF, 0.5 mL HNO_3 and 1.5 mL HCl were added, the sealed bombs were then placed in an electric oven and heated to 180°C for about 12 h. After cooling, the bombs were heated on a hot plate to evaporate to dryness, then 1 mL HNO_3 and 1 mL H_2O were ad-

Table 1. Location and mineralogy description of ferromanganese nodules and crusts from SCS

Station	North latitude	East longitude	Depth/m	Type	Mineralogy	Source
05E105	20°37.256′	116°21.543′	472	nodule	Goethite, quartz, clay minerals, CFA	this study
05E202	20°10.074′	118°44.856′	2 893	nodule	Goethite, quartz, clay minerals	
05E204	20°59.130′	117°57.087′	1 370	nodule	Goethite, barite, pyrite, quartz and clay minerals	
10E204B	21°0.162 9′	117°57.314 2′	1 331	nodule	Goethite, quartz, clay minerals	
ZX31	21°32.79	118°0.59′	1 181	nodule	Goethite, barite, quartz, clay minerals	
05E107	19°46.430′	117°9.528′	2 255	nodule	Todorokite, birnessite, quartz, albite	
09KJ22	17°1.591′	112°59.716′	1 501	nodule	CFA, asbolane, todorokite, birnessite, barite	
J-158	17°33.696′	117°45.206′	3 570	nodule	Birnessite, todorokite and asbolane	
SO4-7DG	17°03′	115°24′	1 200	nodule	10 Å manganates, MnO_2	Zhang et al. (2012)
SO4-1DG	17°54.912 2′	113°5.385 7′	1 700	nodule	Vernadite, quartz, chlorite, illite, albite	
SO4-12DG	15°34.320 2′	116°9.560 2′	1 290	nodule	Quartz, vernadite, mica, calcite, illite, smectite	
KD18	18°28′	115°21′	3 400	nodule	10 Å manganates, MnO_2	Bao and Li (1993)
KD20	17°01′	115°24′	1 070	nodule	10 Å manganates, MnO_2	
KD23	16°46′	114°36′	1 400	nodule	10 Å manganates, MnO_2	
KD35	17°01′	113°03′	1 500	nodule	10 Å manganates, MnO_2	
KD17	18°54′	115°21′	2 470	crust	10 Å manganates, MnO_2	
KD21	16°56′	114°23′	2 170	crust	10 Å manganates, MnO_2	
KD29	16°04′	114°58′	1 250	crust	10 Å manganates, MnO_2	
S-9	15°00′	118°30′	1 000	crust		Wang et al. (1984)
S-10	14°00′	115°06′	3 000	crust		
Xianbei	16°40′	116°50′	3 000	crust	Manganite and MnO_2, feldspar and calcite	Chen and Gui (1998)
Jianfeng	19°28′	116°25′	1 500	crust	Todorokite, MnO_2, bernadite, birnessite	Liang et al. (1991)
NS-52	10°9.48′	113°19.20′	1 700	crust		Chen et al. (2006b)
NS-57	9°16.38′	111°28.62′	978	crust		

ded. The bomb was again sealed and placed in an electric oven at 150°C for about 12 h to dissolve the residue. Major elements were determined using a Thermo-Fisher IRIS II Intrepid XSP ICP-OES. Trace elements and REEs were determined using a Perkin-Elmer ELAN 9000 ICP-MS. All the samples were analyzed at the Institute of Oceanology, Chinese Academy of Sciences (IOCAS).

The sensitivity of the instrument was adjusted to about 30 000 s^{-1} for 1 ng/mL medium-155. The analysis of the reference materials (GBW07315, GBW07316, BCR-2, BHVO-2, GBW0725, GBW07296, NOD-P-1 and NOD-A-1) which are either sediment, basalt or manganese nodules, agree well with the certified value. The accuracies of the analyses are estimated to be better than ±5%–10% (relative) for most elements.

3 Results and discussion

3.1 *REE distribution characteristics in ferromanganese deposits*

3.1.1 *REE content, mineralogical composition and geographical distribution*

The REEs are conventionally subdivided into light REEs (LREE: La to Sm) and heavy REEs (HREE: Eu to Lu and Y) (Kato et al., 2011). The ferromanganese deposits mainly formed of Mn-oxides intergrown with Fe oxyhydroxides, are a potential source of REE (Hein et al., 2013). High concentrations of the REY, up to 3 000×10^{-6} total REY, comparable with the level in ore deposits in southern China, are reported for ferromanganese crust-nodule deposits from the Shatsky Rise, Northwest Pacific (Hein et al., 2012).

The SCS developed from continental margin rift to ocean basin with an area of 3.5×10^6 km^2 and a maximal depth of 5 500 m (Fig. 1). Ferromanganese oxide deposits from the SCS are found in a wide variety of oceanographic and tectonic settings such as the northeastern slope, northwestern and central basin (Fig. 1) (Lin et al., 2003; Zhang et al., 2012; Zhong et al., 2017a). On the basis of their morphology and size, ferromanganese oxide deposits can be divided into ferromanganese crusts, polymetallic nodules, and micronodules (<1 mm in diameter). Ferromanganese micronodules are an important reservoir for Mn and associated transition elements in oxic deep-sea sediments (Stoffers et al., 1984). The abundance of micronodules seems to be correlated reciprocally with the sedimentation rate and highest abundance occurring in dark brown clay where the sedimentation rate is very low (Banerjee and Iyer, 1991; Chauhan, 2003; Dekov et al., 2003; Duliu et al., 2009). They tend to predominate in the coarse fraction of the surface sediment and spread unevenly, especially in the eastern deep basin (Fig. 2). According to percentage composition of micronodules concentrated in the coarse silt sediment, it can be divided into a high content area, a middle content area and a low content area. The distribution of ferromanganese nodules and crusts controlled by the distribution trend of micronodules, are roughly parallel to the NE-striking faults.

Combined with mineral composition (Fig. 3 and Table 1), most of ferromanganese crusts, essentially composed of todorokite, are widely distributed on the volcanic seamounts which formed after the cessation of the sea floor spreading in the basin (Fig. 1), such as the Daimao Seamount (Sta. 8), the Xianbei Seamount (Sta. Xianbei), and the Zhenbei Seamount (Sta. 9). On the other hand, they also spread on the lower continental slope, such as the Jianfeng Seamount, the Shuangfeng Seamount (Sta. KD17), the Zhongsha and Xisha platforms (Stas KD21 and KD29). The content of LREE in the polymetallic nodules/crusts is obviously higher than that of HREE, with the total LREE ranging from 50.5×10^{-6} to 2 584.3×10^{-6}. There are four stations (such as Stas KD20, KD18, Xianbei and NS57) found on the slope and southern subbasin area, whose REE content is more than 2 000×10^{-6}. Most of nodules with the total LREE content are larger than 1 000×10^{-6}, appearing mainly in the Zhongsha and Xisha plat-

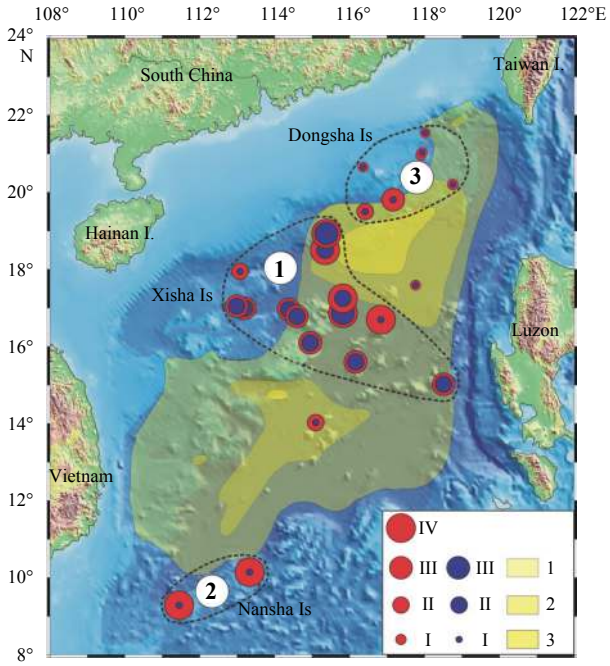

Fig. 2. Prospecting zones and divisions of rare earth placer deposits in ferromanganese nodules (crusts) from SCS. 1. The high content area; 2. general content area; and 3. low content area (modified from Chen et al. (2006a)). The red circle represents the LREE oxide value and the blue circle represents the HREE oxide value. LREE and HREE oxide values mentioned in the paper on which Table 5 is based. The yellow zones represents the content distribution of micronodules.

forms and spreading sparsely on the southwest subbasin. The high contents of REEs normally are in relation with hydrogenesis and the abundance of vernadite. The nodules with the total LREE content is less than 1 000×10^{-6}, are mainly distributed in the northeastern SCS. And the minimum value appears in Sta. 05E202 of the northeastern SCS (Fig. 4c). These nodules have a pristine mineralogy formed by pyrite and barite which cannot accumulate REEs (Fig. 3 and Table 1). The total HREE content ranges from 18.6×10^{-6} to 442×10^{-6}, which is much smaller than that of the total LREE, indicating that the polymetallic nodules in the SCS are dominated by the total LREE (Fig. 4d). REY range from 69.1×10^{-6} to 2 919×10^{-6}, and the maximum appears at the Sta. KD18 in the deep sea basin, and the minimum also appears at the Sta. 05E202 in the northeastern SCS (Fig. 4a). The high and low value distributions of the total HREE and REY are basically consistent with the distribution of the total LREE: the high-value area is located on the slope of the Zhongsha and Xisha Islands, the low-value area is located on the northeastern slope.

3.1.2 *Ce enrichment*

Ce has been widely applied for catalytic converters in cars, petroleum refining, steel production, corrosion protection, carbon arc lamps, and cigarette lighter flints (Dutta et al., 2016). As is also the most abundant natural element in lanthanide elements, the Ce content of the polymetallic nodules/crusts in the SCS ranges from 22.43×10^{-6} to 2 040×10^{-6}, accounting for almost 60% of the total REE content. The maximum value appears at the Sta. KD18 at the deep sea basin and the minimum value appears at Sta. 05E202 in the northeastern SCS. These high value areas are mainly distributed on the island slope of Zhongsha and Xisha platforms (c(Ce)=642×10^{-6}–2 040×10^{-6}) (Fig. 4b). Most of Ce contents are within the scope of 900×10^{-6}–2 000×10^{-6}, which is basically consistent with the distribution of the total HREE, REY, and LREE. The distribution relatively to water depth is similar to that of the ratio of LREE content to HREE one and Ce anomaly ratios in the deposits (Fig. 5). However, the correlation coefficient between Ce and water depth is only 0.01 and the strong positive Ce anomalies in nodules and crusts from the SCS imply that Ce in deposits come from seawater (Fig. 5). The correlation coefficients between Ce and Fe, Mn are –0.60 and 0.68, respectively (Table 2). Ce enrichment in nodules and crusts depends on a preferential fractionation to the Fe and Mn phases, with a slight relative preference for Fe oxyhydroxides (Table 2) (Hein et al., 1988; Bau and Koschinsky, 2009). The results provided by these authors indicate that the transfer of Ce from seawater does not occur via a discrete solid Ce (IV) oxide phase from dissolved Ce (III), but rather Ce dissolved in waters remains trivalent and its oxidation to the tetravalent form occurs at the surface of Fe-Mn oxyhydroxides after its sorption into their structure (Fig. 6). Therefore, the Ce element may be the first REE separated and extracted from sedimentary mineral resources in the ocean in the future.

3.2 *Comparison with other marine REY-rich deposits*

The deep-sea REY-rich deposits of polymetallic nodules, Co-rich crusts and soft mud are reported from many parts of the world (Rona, 2008) (Fig. 7). The SCS is an important tectonic unit of the western Pacific Ocean active continental margins. Because of the enormous amount of terrigenous sediment input into marginal seas, Fe- and Mn-oxide precipitates are easily diluted making it difficult to enrich metals of potential economic interest, and deposits can be buried quickly by sediments (Zhang et al., 2013). However, the enrichment of REE and Ce in polymetallic nodules and crusts in the SCS provides a good premise for the comprehensive development of seabed mineral resources.

The SCS deposits are characterized by Fe-oxyhydroxides predominating over Mn-oxides, which in samples from the Pacific Ocean the Mn oxide vernadite is predominant (Hein et al., 2012). This predominance of goethite-family minerals in the SCS deposits is similar to other locations from the Philippine area (Xu et al., 2006). Quartz grains and other clay minerals, abundant in the deposits can be probably related to the terrigenous input, as has been found for crusts from the California continental-margin (Conrad et al., 2017). A comparison between REY contents in the SCS samples and other ferromanganese deposits and deep-sea mud from other oceans is provided in Fig. 8. The maximum total REY content of the polymetallic nodule/crust in the SCS is lower than that of the Northwest Pacific (Hein et al., 2012) and California marginal sea (Conrad et al., 2017), but similar to the total REY of the Northeast Atlantic (Muinos et al., 2013) and southern Pacific nodules (Hein et al., 2015). Especially, the total REY of the SCS (c(REY)=69×10^{-6}–2 919×10^{-6}) were significantly higher than that in the central Pacific Basin (Cui et al., 2009) and the Philippine Sea (Xu et al., 2006). At the same time, the maximum total REY content value of polymetallic nodule/crust in the SCS is also significantly higher than that in the eastern Pacific Ocean CCFZ, southeastern Pacific and western Pacific mud. In regard to Ce content, the maximum content in the SCS is the same as that in the southern Pacific, which is lower than that in the Northwest Pacific (Hein et al., 2012) and the California marginal sea (Conrad et al., 2017), but higher than that in the Central Indian Basin (Cui et al., 2009), the northeastern Atlantic (Muinos et al., 2013), the Philippine Sea (Xu et al., 2006) and the central Pacific Basin.

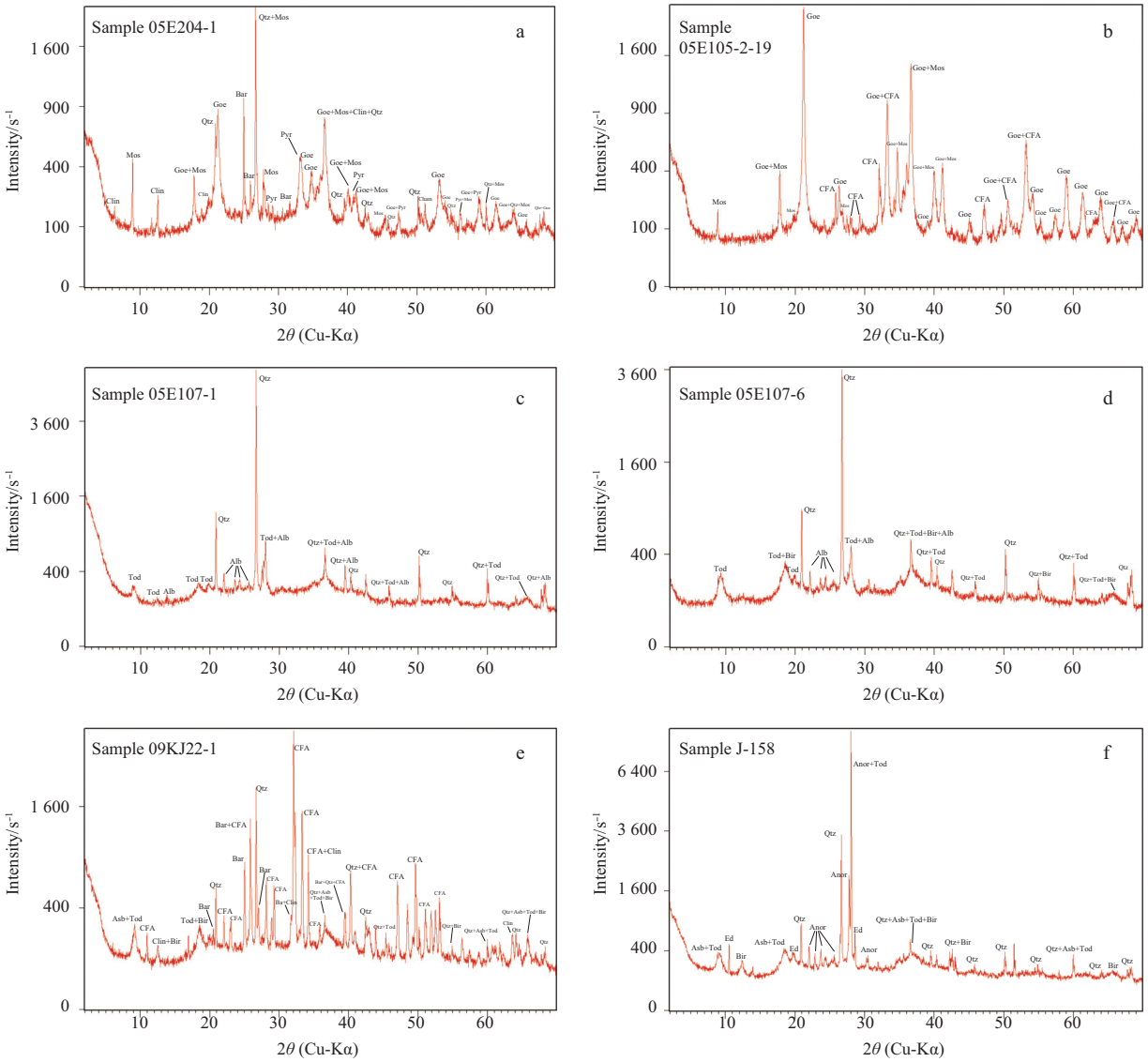

Fig. 3. The XRD profiles for ferromanganese nodules from the SCS. Qtz represents quartz, CFA carbonate fluorapatite, Tod todorokite, Bir birnessite, Asb asbolane, Goe goethite, Bar barite, Pyr pyrite, Mos muscovite, Alb albite, Anor anorthite, Clin clinochlore, and Ed edentate (amphibole).

Therefore, the rare earth resources in seabed polymetallic nodules and Co-rich crusts have attracted the attention of the international seabed authority and governments. Since the development of submarine technology, a research into ferromanganese nodules and crusts has become more sophisticated. Especially, the production cost and difficulty of rare earth resource in polymetallic nodules and crusts in the SCS are less than that in the deep-sea basin because they mainly occur at comparatively shallow depth, forming along the continental margin (Conrad et al., 2017; González et al., 2016; Marino et al., 2017). Moreover, the resource potential and economic value of the REEs, especially Ce, are much larger than those central Pacific Basin, the CCFZ in the eastern Pacific (Wegorzewski and Kuhn, 2014) and the Indian Ocean Basin (Pattan and Parthiban, 2011) where China participates in the exploration or attention.

3.3 *Main factors affecting the Ferromanganese deposits and REY distribution*

Many ferromanganese deposits from different parts of the world oceans have been studied extensively (Calvert, 1978; Aplin and Cronan, 1985; Bau et al., 1996; Hein et al., 1997; Mills et al., 2001; Koschinsky and Hein, 2003; Rajani et al., 2005). Traditionally, hydrogenous precipitate from sea water, whereas diagenetic nodules form from metal ions in sub-oxic pore waters, and hydrothermal nodules form from metals supplied by hydrothermal vent fluids (Bau et al., 2014). Ferromanganese deposits of different genetic origins are characterized by distinctive composition of REEs (Byrne and Kim, 1990; German and Elderfield, 1990). In addition, several factors such as the rate of precipitation, nature of geochemical components in oxides, speciation of elements from sea water and hydrothermal fluid are major cause of such compositional variations (Koschinsky and Halbach, 1995; Bau and Dulski, 1996; Koschinsky et al., 1996; Takahashi et al., 2007).

To better quantify and understand the processes that control the REY composition of the ferromanganese deposit samples, the elemental data were subjected to a statistical factor analysis. The results of this analysis are shown in Tables 2 and 3. Differences in the chemical composition of the ferromanganese deposit

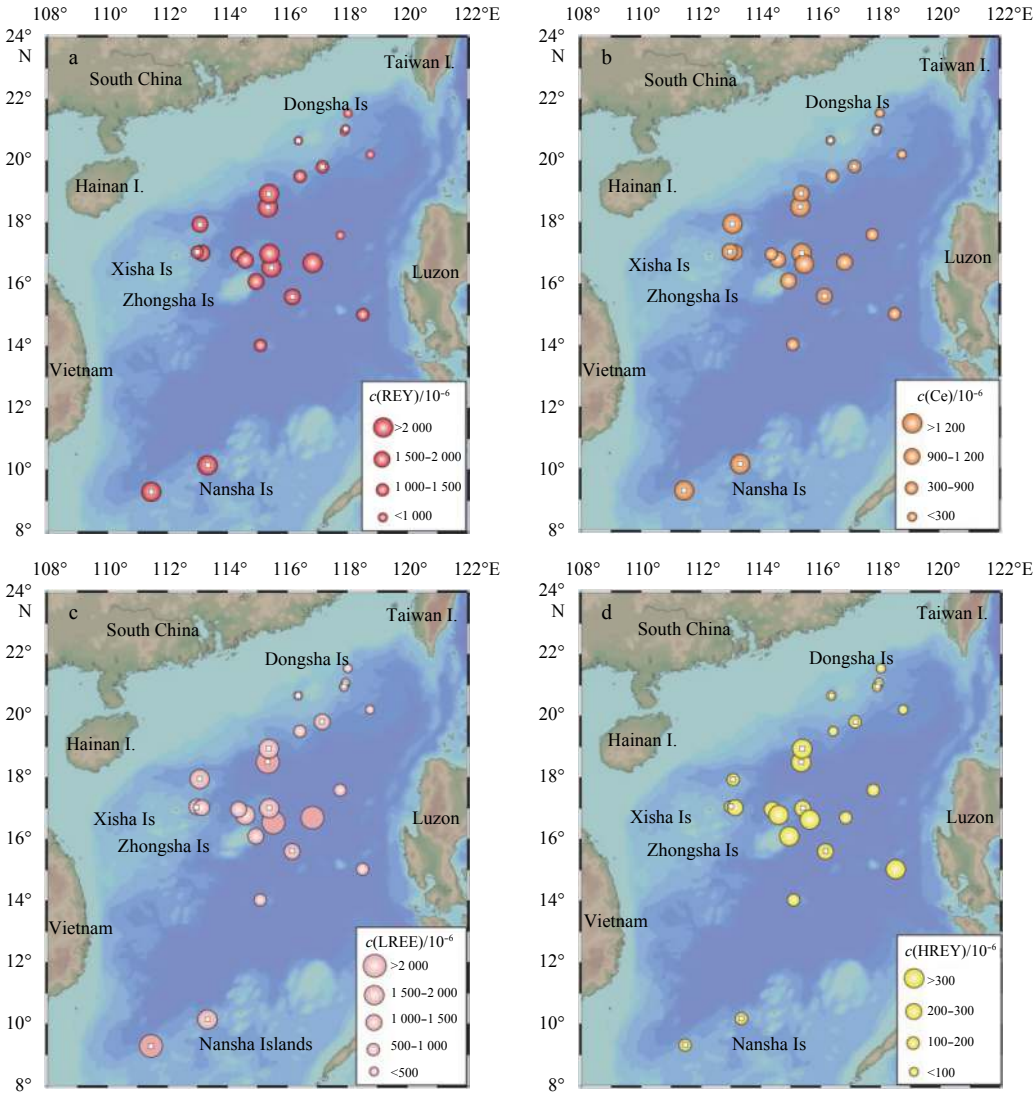

Fig. 4. Distribution characteristics of REY content in the ferromanganese nodules from the SCS (a), distribution characteristics of Ce content in the ferromanganese nodules from the SCS (b), distribution characteristics of LREE content in the ferromanganese nodules from the SCS (c), and distribution characteristics of HREE content in the ferromanganese nodules from the SCS (d).

samples can be accounted for statistically by changes in the relative proportions of three principal factors [with eigenvalues, or sums of squared (SS) loadings, of being greater than 1] which together account for 82% of the sample variance. The total REY concentrations are positively correlated with Ti which is enriched in detrital minerals; titanium mainly forms a hydrogenetic phase, probably consisting of TiO_2*H_2O intergrowth with the amorphous FeOOH phase (Koschinsky and Hein, 2003). The factor analysis reveals that the REY are also located in association with Mn, Fe, Cu, Co and Ni that are generally considered have a significant hydrogenous source in the ferromanganese deposits (Koschinsky and Halbach, 1995). Uptake of REY from seawater is widely considered to occur via scavenging by Fe-Mn oxide phases (Piper, 1974; German et al., 1991; Bau and Koschinsky, 2009). Sequential leaching of some samples reveals that REEs and yttrium are mainly associated with Fe-Mn oxyhydroxide phase, both Mn-oxide and Fe-oxyhydroxide phases contain the major fraction of these elements (Zhong et al., 2017b), which is consistent with comparative study of hydrogenous and hydrothermal deposits collected from two seamounts in the Andaman Sea (Prakash et al., 2012).

On the other hand, the degree of enrichment of REY is related to a genetic model and nodules and crusts growth rates (Bau and Koschinsky, 2009). Different types of ferromanganese deposits can be distinguished by the field on which they plot on a Mn-Fe-(Cu+Co+Ni) ternary diagram, which delimitates the diagenetic, hydrogenous and hydrothermal fields according to the relative proportions of these groups of elements. Compared with the geochemical values of typical oceanic diagenetic nodules from the CCFZ (Wegorzewski and Kuhn, 2014) and hydrogenetic-diagenetic nodules from the Indian Ocean (Pattan and Parthiban, 2011), most of the nodules and crusts from the SCS fall within the hydrogenetic field on this ternary diagram (Fig. 9) in an area superimposed by other samples from the Philippine Sea (He, 1991; Xu et al., 2006) and more enriched in Fe than the crusts from the northwestern Pacific Ocean (Hein et al., 2012). It is consistent with previous reported results of ferromanganese nodules and crusts found in the SCS (Bao and Li, 1993; Chen and Gui, 1998; Chen et al., 2006a). Hydrogenesis via very slow growth rates (1–2 mm/Ma) allows REY to accumulate in ferromanganese oxy-

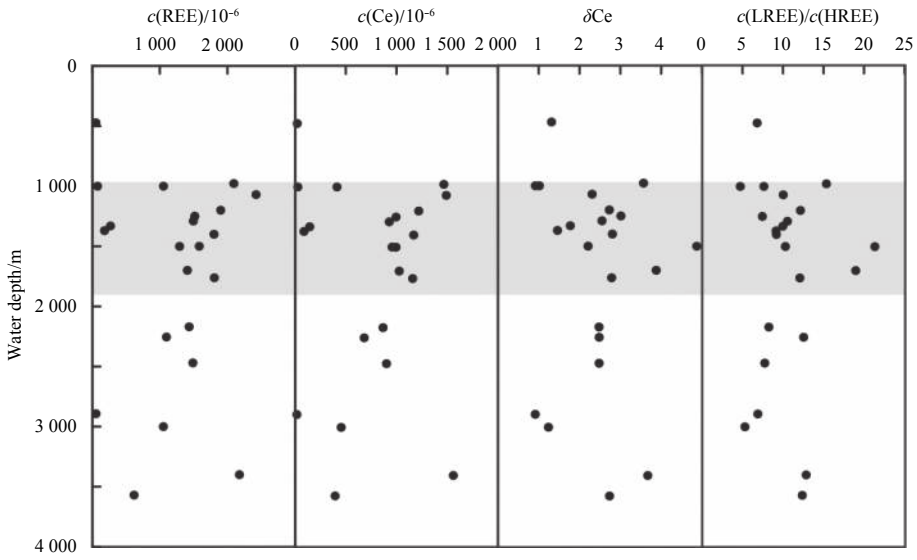

Fig. 5. Depth relations of the total REE, Ce contents and Ce anomaly, the ratio of LREE content to HREE one (shaded zone is the high REE content area).

hydroxide structures on nodules and crusts surfaces. According to Sholkovitz et al. (1994) and Moffett (1990), this enrichment is strongly dependent on time in which ferromanganese minerals are in contact with sea water, therefore supporting the control of growth rates.

However, the study nodules and previous data present the ratio of Mn/Fe < 0.25 and low contents of Co, Ni, Cu and REE in the Dongsha Islands. The diagram discriminate these nodules as diagenetic in origin, but overlaps slightly with the hydrothermal field (Fig. 8). Abundant references report on nodules from shallow waters and continental margins where Fe, Mn and trace metals contents are rather similar to these Fe-rich nodules from the Dongsha Islands (Calvert, 1978; Glasby et al., 1997; Baturin et al., 2002). They all display very low Mn/Fe ratios as a result of their fast growth rates by combined diagenetic-hydrogenous processes. In this sense, fast growth rates emphasize the importance of sediment diagenetic processes (Reyss et al., 1982). This relatively rapid accumulation is one of the main causes for the overall low content of rare earth metals in these nodules.

3.4 *Resource potential of SCS ferromanganese deposits*

3.4.1 *Classification standard of REY sources of ferromanganese deposits*

The deep-sea mud, polymetallic nodules and Co-rich crusts are enriched in rare earth elements, but no exact resource grade standard system has been established. Huang et al. (2014) proposed classification criteria for rare earth resources in deep-sea sediments. However, the REY value of the ferromanganese nodules and crusts has not been yet proposed exact quantitative criteria. Usually, the industrial evaluation of land rare-earth minerals takes the form of measuring an oxide content. In this paper, according to "land-based REE mines exploration norms" (Industrial standard, DZ/T 0204–2002), referring to the industrial grade of land-based weathering crust ion-adsorption rare earth mining: the border grade of LREE is 700×10^{-6} rare earth oxides (REO) and its industrial grade reaches $1\,000\times10^{-6}$ REO; border grade of HREE is 300×10^{-6} REO and its industrial grade reaches 500×10^{-6} REO.

According to the above classification standard, the measured REE content is converted into the REO content, LREE and HREE of the ferromanganese deposits in the study area could be divided into four levels, as shown in Table 4.

Ⅰ. Non-enriched type: REO content is less than or equal to the border grade;

Ⅱ. weakly enriched type: REO content is greater than the border grade, less than or equal to industrial grade;

Ⅲ. enriched type: REO content is greater than the industrial grade, less than or equal to two times of industrial grade;

Ⅳ. extremely enriched type: REO content is more than two times of the industrial grade.

3.4.2 *Quality characteristics of REO deposits and its resource perspective*

In this study, the REEs should be converted to oxidation level and likely to be close to the industrial grade because the current measurement only examines single element. On the basis of the classification standard in Table 4, if there are more than one datum at one station, each datum is classified by the grade level, the level of most data is taken as this station's level. In addition to REE, ferromanganese deposits have long been considered a potential resource for metals, such as Ni, Co, Co and Li, that are important in contemporary technology (Hein et al., 2013). If the account of level of different data is consistent, comprehensively taking into account of other metals, the maximum level is taken as this station's grade. As shown in Table 5 and Fig. 2, the LREE in the ferromanganese deposits from the SCS is relatively enriched. There are nine enriched type stations and seven extremely enriched type stations, respectively. The most abundant station is KD18, with the REO content is $3\,145\times10^{-6}$, more than three times of the industrial grade, which appears on the island slope of the Xisha and Zhongsha platforms. The non-enriched station is 05E202 (the REO content is 60.5×10^{-6}), distributed on the northeastern slope. Compared with the LREE, HREE of ferromanganese nodules and crusts is not enriched. Non-enriched and enriched stations account for 54% and 38% of the total stations, respectively. The most abundant station is KD17, with the REO content is 532.4×10^{-6}, which is slightly higher than the industrial

Table 2. Correlation coefficients between elements in ferromanganese deposits

	Al	Ca	K	Mg	Fe	Mn	Na	P	Ti	Co	Ni	Cu	La	Ce	Pr	Nd	Sm	Eu	Gd	Tb	Dy	Ho	Er	Tm	Yb	Lu	Y	REY
Al																												
Ca	–0.21																											
K	**0.72**	0.01																										
Mg	**0.50**	0.04	0.26																									
Fe	**–0.49**	–0.27	–0.40	**–0.42**																								
Mn	0.21	0.32	0.04	**0.53**	**–0.87**																							
Na	0.33	0.18	0.15	**0.43**	**–0.87**	**0.88**																						
P	–0.35	**0.88**	–0.05	–0.14	0.09	–0.07	–0.21																					
Ti	0.12	0.18	–0.11	0.19	**–0.46**	**0.58**	**0.66**	–0.21																				
Co	–0.11	0.15	–0.25	**0.42**	**–0.60**	**0.79**	**0.74**	–0.15	**0.57**																			
Ni	**0.45**	0.15	0.32	**0.69**	**–0.75**	**0.80**	**0.68**	–0.14	0.36	**0.52**																		
Cu	0.29	0.12	–0.01	0.17	–0.26	0.36	0.38	–0.15	**0.73**	0.13	0.25																	
La	–0.18	0.09	–0.23	–0.06	–0.39	**0.50**	**0.59**	–0.17	**0.58**	**0.65**	0.22	0.25																
Ce	0.04	0.32	–0.12	0.12	**–0.60**	**0.68**	**0.75**	–0.01	**0.80**	**0.60**	0.37	**0.55**	**0.53**															
Pr	–0.05	0.14	–0.26	0.06	**–0.58**	**0.76**	**0.76**	–0.22	**0.76**	**0.67**	0.40	**0.50**	**0.98**	**0.82**														
Nd	–0.09	0.12	–0.24	0.06	**–0.64**	**0.78**	**0.81**	–0.23	**0.64**	**0.74**	**0.42**	0.31	**0.79**	**0.76**	**0.96**													
Sm	–0.06	0.12	–0.28	0.06	**–0.58**	**0.76**	**0.76**	–0.26	**0.77**	**0.67**	0.40	**0.53**	**0.68**	**0.80**	**0.99**	**0.94**												
Eu	–0.05	0.09	–0.32	0.03	**–0.51**	**0.70**	**0.67**	–0.27	**0.76**	**0.60**	0.35	**0.55**	**0.60**	**0.74**	**0.96**	**0.86**	**0.97**											
Gd	–0.08	0.13	–0.33	0.02	**–0.56**	**0.74**	**0.72**	–0.23	**0.75**	**0.66**	0.36	**0.50**	**0.66**	**0.76**	**0.98**	**0.91**	**0.99**	**0.98**										
Tb	–0.01	0.08	–0.29	0.10	**–0.50**	**0.69**	**0.70**	–0.26	**0.71**	**0.61**	0.37	**0.53**	**0.62**	**0.62**	**0.88**	**0.82**	**0.91**	**0.93**	**0.93**									
Dy	–0.03	0.10	–0.31	0.07	**–0.43**	**0.65**	**0.62**	–0.27	**0.86**	**0.57**	0.32	**0.67**	**0.89**	**0.72**	**0.92**	**0.80**	**0.94**	**0.96**	**0.95**	**0.91**								
Ho	–0.14	0.03	–0.31	–0.03	**–0.46**	**0.62**	**0.59**	–0.25	**0.49**	**0.64**	0.21	0.23	**0.65**	**0.48**	**0.77**	**0.77**	**0.79**	**0.82**	**0.83**	**0.84**	**0.74**							
Er	–0.09	0.09	–0.37	0.08	**–0.48**	**0.71**	**0.68**	–0.26	**0.75**	**0.67**	0.33	**0.53**	**0.92**	**0.71**	**0.94**	**0.86**	**0.96**	**0.98**	**0.98**	**0.95**	**0.96**	**0.86**						
Tm	0.03	0.12	–0.26	0.12	–0.34	**0.53**	**0.55**	–0.22	**0.88**	**0.51**	0.29	**0.69**	**0.49**	**0.65**	**0.77**	**0.60**	**0.79**	**0.84**	**0.81**	**0.85**	**0.92**	**0.62**	**0.86**					
Yb	–0.15	0.07	–0.37	–0.02	**–0.46**	**0.66**	**0.63**	–0.26	**0.68**	**0.67**	0.25	**0.44**	**0.68**	**0.61**	**0.89**	**0.83**	**0.90**	**0.92**	**0.94**	**0.92**	**0.91**	**0.93**	**0.96**	**0.80**				
Lu	0.002	0.12	–0.27	0.09	–0.34	**0.54**	**0.55**	–0.23	**0.86**	**0.51**	0.28	**0.70**	**0.47**	**0.65**	**0.81**	**0.63**	**0.82**	**0.86**	**0.84**	**0.87**	**0.95**	**0.63**	**0.89**	**0.98**	**0.84**			
Y	–0.18	0.36	–0.31	0.02	**–0.45**	**0.63**	**0.54**	0.08	**0.63**	**0.60**	0.33	**0.44**	**0.74**	**0.60**	**0.78**	**0.72**	**0.78**	**0.79**	**0.81**	**0.76**	**0.78**	**0.69**	**0.80**	**0.69**	**0.79**	**0.73**		
REY	–0.04	0.28	–0.21	0.08	**–0.62**	**0.75**	**0.80**	–0.09	**0.83**	**0.70**	0.39	**0.55**	**0.69**	**0.96**	**0.93**	**0.89**	**0.92**	**0.86**	**0.89**	**0.77**	**0.84**	**0.65**	**0.84**	**0.74**	**0.77**	**0.75**	**0.73**	

Note: Significant ($P < 0.05$) correlations are highlighted in bold face.

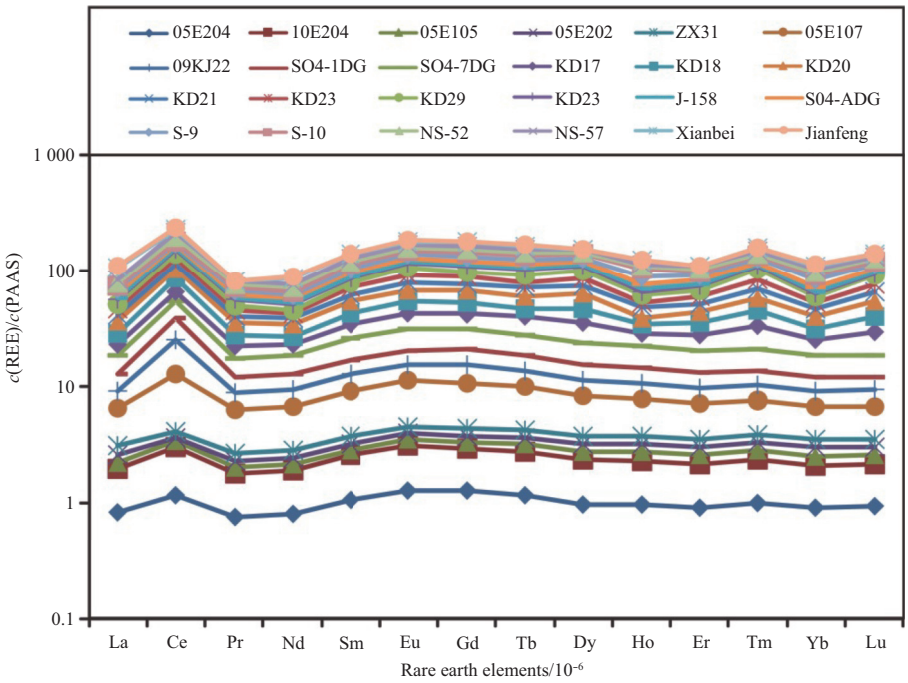

Fig. 6. REE shale (PAAS)-normalized patterns of the study and other SCS nodules/crusts.

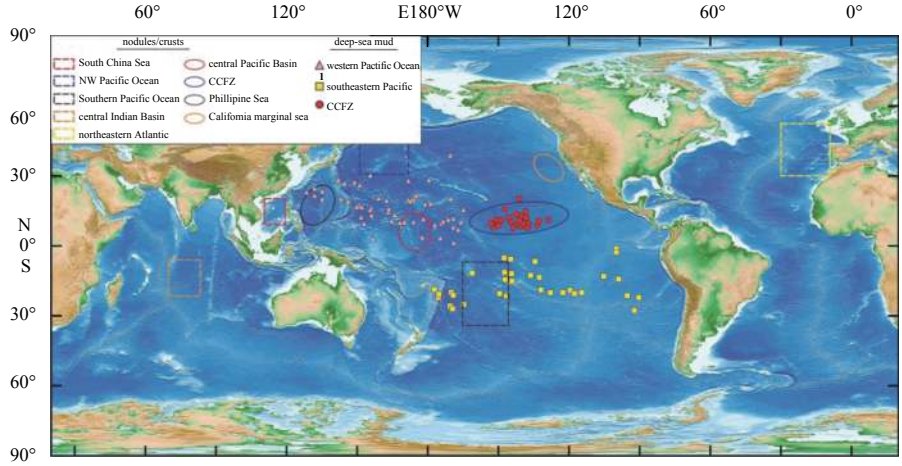

Fig. 7. Map of all well-study areas for marine ferromanganese deposits and deep-sea mud.

grade value. And the lowest w(REO) value is 27.2×10^{-6}, far below the border grade, also located on the northeastern slope. Combined with topography and formation environment, according to the LREE and HREE grade level of the SCS sample stations, the rare earth resources of ferromanganese nodules and crusts from the South China Sea are divided into three prospective areas (Fig. 2).

(1) Zhongsha and Xisha platform-deep central basin prospective area. The prospective fields are distributed on the northern slope of the SCS where the Pacific Ocean deep water (PDW) influence is stronger. The basin-scale oxygen distribution suggests that the PDW intrudes into the SCS through the Luzon Strait, and is transported north and westward, and then southward along its western margin (Qu et al., 2006). These currents, which are strongest along the SCS slope, promote nodules and crusts formation, enhance turbulent mixing, and produce upwelling, leading to increased primary productivity and the maintenance of an oxygen minimum zone (Hein et al., 2010). In hydrogenetic ferromanganese nodules and crusts, the trace elements appear to be selectively distributed between Mn oxide and Fe oxide phases. It is characterized by extremely enriched LREE resource. And the majority stations are enriched with HREE, higher than the border grade value. Although their distribution is not consistent with the high content area of micro-nodules and micro-crusts and is distributed in low-content areas. According to the comparative study of nodules and micro-nodules, the high content of micro-nodules and crusts appears in the northeastern deep-sea basin, which is consistent with the high value area of REE of fine-grained fraction of the surface sediment (Fig. 2) (Liu et al., 2010a). They can not reach the border grade. Therefore, the Xisha and Zhongsha platform-central deep basin area shows a significant resource potential for these rare earth metals due to their high nodule abundance, and high enrichment.

(2) Southern slope of the southwest sub-basin prospective

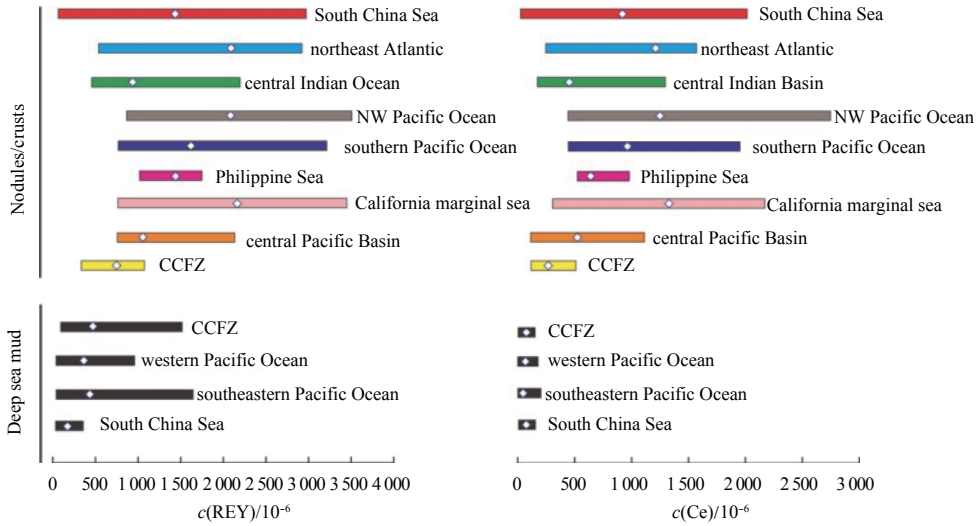

Fig. 8. Comparison of REY and Ce contents of the ferromanganese nodules (crusts) and deep-sea mud in different oceans and seas.

Table 3. Varimax rotated factor matrix for SCS ferromanganese deposes

	Factor 1	Factor 2	Factor 3
Al	–0.122	**0.783**	–0.410
Ca	0.115	0.090	**0.906**
Fe	–0.457	**–0.796**	–0.203
K	–0.391	**0.693**	–0.108
Mg	0.037	**0.752**	–0.038
Mn	**0.684**	0.626	0.267
Na	**0.668**	0.661	0.105
P	–0.232	–0.160	**0.902**
Ti	**0.814**	0.212	–0.071
Co	**0.670**	0.359	0.213
Ni	0.313	**0.814**	0.083
Cu	0.585	0.157	–0.208
La	**0.945**	0.139	0.074
Ce	**0.795**	0.256	0.221
Pr	**0.962**	0.139	0.065
Nd	**0.879**	0.223	0.123
Sm	**0.970**	0.140	0.026
Eu	**0.977**	0.061	–0.031
Gd	**0.981**	0.084	0.041
Tb	**0.929**	0.104	–0.067
Dy	**0.972**	0.028	–0.082
Ho	**0.840**	0.017	0.012
Er	**0.987**	0.034	–0.020
Tm	**0.867**	0.035	–0.134
Yb	**0.955**	–0.016	–0.017
Lu	**0.901**	0.008	–0.122
Y	**0.815**	0.006	0.296
REY	**0.903**	0.211	0.187
Eigen Value (SS loading)	16.435	4.259	2.285
Total variance/%	58.695	15.210	8.162
Acum. Variance/%	58.695	73.905	82.068

Note: Numbers in bold face denote the values of elements that appear to be loaded in the factor.

area. There are only two stations (NS52 and NS57) in this area. Unlike the low concentration (143×10^{-6}–200×10^{-6}) of HREE, the content of LREE oxides ranges between $2\,279\times10^{-6}$ and $2\,411\times10^{-6}$, which falls into extremely enriched type. The prospective area is located on the western island of the southwestern subbasin, where crusts are found to be growing together with phosphate rocks (Chen et al., 2006b). It is generally known that apatite is one of the most critical mineral species, which can acquire REY from a wide variety of sea water occurring on the sea floor of continental shelves and slopes along the western continental margins of the Pacific and Atlantic Oceans (Hucrrns et al., 1991; Hughes and Rakovan, 2015). Marine phosphorites deposits are known to concentrate REY during early diagenetic formation (Hein et al., 2016). In general, the discovery and delineation of the prospective area break through the limitations of understanding on previous knowledge of distribution, but the formation mechanism of these crusts needs to further study.

(3) Northeast slope prospective area. Fe-rich nodules in the SCS were first collected on the northeastern slope, however, detailed geochemical studies about the total REY contents are still limited, and the systematization and the regularity are not evident in this area, so the results could not reflect its potential distribution of rare earth. The ferromanganese nodules shaped by rod, rodlike, spherical and block type, covered under the shallow mud in this area. The minimum values of light and heavy rare earth oxides in ferromanganese nodules are found in this area, and the heavy and light rare earths are characterized by non-enriched and weakly enriched type. The economic value of rare earth resources is not great, but its Fe content is very high. Within the study area, the widespread faults systems of the Dongsha Islands are the main migration system of fractured conduits or channels for gas and methane bearing fluids migrate from the deep parts of the basin into shallow sediments (Hui et al., 2016). It needs to further study whether the Fe-rich nodules on the northeastern slope of the SCS with high Fe content, low Mn content (c(Mn)/c(Fe) = 0.02) and low trace metals content and rare earth elements are closely related to leakage of cold spring fluid.

4 Conclusions

The REY enrichment in ferromanganese deposits from the SCS has high potential for economic interests. Overall, the contents and distribution of REY in the ferromanganese nodules and crusts from the SCS show a geographic variation. REY is essentially enriched in LREE. High REY content peak in the Xisha Is-

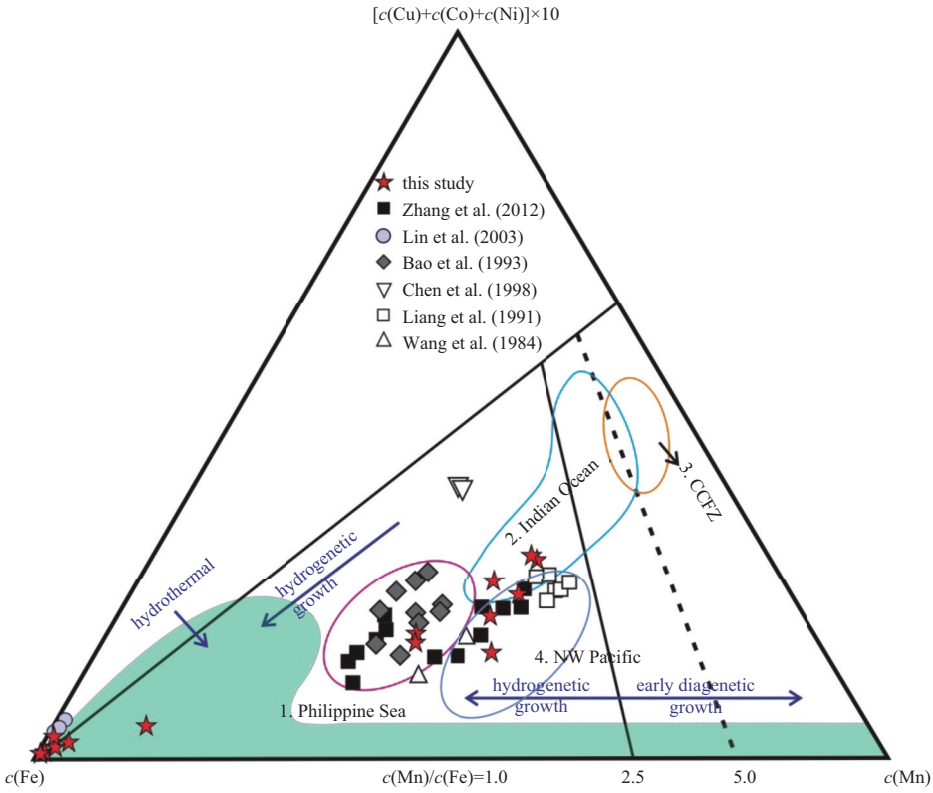

Fig. 9. Ternary plots for SCS nodules and crusts and other ferromanganese deposits from the the Philippine Sea (He, 1991; Xu et al., 2006), Indian Ocean (Mukhopadhyay et al., 2003), NW(northwestern) Pacific (Hein et al., 2012) and CCFZ (Wegorzewski and Kuhn, 2014); ternary diagram modified from Bonatti et al. (1972).

Table 4. The abundance and classifications of rare earth elements in the ferromanganese nodules and crusts

Category grade	Enrichment type	LREE	Location	HREE	Location
		c(REO)/10^{-6}		c(REO)/10^{-6}	
Ⅰ	non-enriched	∑LREE<700	6	∑HREE<300	13
Ⅱ	weak enrichment	700<∑LREE<1 000	2	300<∑HREE<500	9
Ⅲ	enriched	1 000<∑LREE<2 000	9	500<∑HREE<1 000	2
Ⅳ	Extremely enriched	∑LREE >2 000	7	∑HREE >1 000	

Table 5. The abundance of characteristic parameters of rare earth elements in ferromanganese nodules/crusts

	Station	05E204	10E204B	05E105	05E107	09KJ22	SCSN1	SCSN7	SCSN12	KD17	KD18	NS52	NS57
	N	2	2	2	5	2	8	2	3	3	2	2	2
c(REY)/10^{-6}	min	164.7	120.4	40.2	928	1 374	861	1 941	1 581	1 098	1 687	1 447	2 001
	max	245.6	482.3	104	1 460	1 489	1 958	2 113	1 660	2 200	2 919	2 166	2 188
	mean	205.2	301.4	72	1 167	1 431	1 466	2 027	1 625	1 629	2 303	1 806	2 094
c(LREE)/10^{-6}	min	129.9	90.6	25.2	814	1 042	792	1 685	1 357	888	1 454	1 343	1 876
	max	200.4	403.5	72.9	1 282	1 427	1 884	1 826	1 383	1 758	2 584	1 992	2 055
	mean	165.2	247	49	1 017	1 235	1 361	1 755	1 366	1 317	2 019	1 667	1 966
c(HREE)/10^{-6}	min	34.8	29.8	15.1	114	61.6	76.4	256	224	210	233	104	124
	max	45.2	78.9	30.9	187	331	161	288	277	422	335	174	133
	mean	40.0	54.3	23.0	150	197	130	272	259	312	284	139	129
c(Ce)/10^{-6}	min	74.0	45.2	11.0	546	810	595	1 193	897	642	1 087	967	1 414
	max	110.2	252.7	41.3	882	1 188	1 431	1 252	987	1 135	2 040	1 358	1 526
	mean	92.1	148.9	26.2	685	999	1 031	1 223	932	905	1 564	1 163	1 470
reference		this study					Zhang et al. (2013)			Bao et al. (1993)		Chen et al. (2006b)	

Note: *N* denotes the amount of samples in one site.

lands, but has lower values in the Dongsha Islands. Our results indicate that the contents of REY depend strictly on the crust mineralogy and especially on the abundance of Fe-oxyhydroxides. On the basis of the criteria of the land-based REE mines, we calculated grades for LREE and HREE in ferromanganese deposits from the SCS. A comprehensive analysis shows that ferroman-

ganese deposits from the Zhongsha and Xisha platform may contain abundant rare metal minerals, with a good prospect as rare metal placer resource, and the hydrocarbon seep may also have good metallogenic prospects in the local area of the Dongsha Islands.

Acknowledgements

The authors are grateful to Usui Akira and Liu Qingsong for their guidance and constructive discussions. This study is benefited from the scientific cooperation between the South China Sea Institute of Oceanology, Chinese Academy Sciences and the Geological Survey of Spain (IGME).

References

Alonso E, Sherman A M, Wallington T J, et al. 2012. Evaluating rare earth element availability: a case with revolutionary demand from clean technologies. EnvFemental Science & Technology, 46(6): 3406–3414

Aplin A C, Cronan D S. 1985. Ferromanganese oxide deposits from the Central Pacific Ocean: II. Nodules and associated sediments. Geochimica et Cosmochimica Acta, 49(2): 437–451

Banerjee R, Iyer S D. 1991. Biogenic influence on the growth of ferromanganese micronodules in the Central Indian Basin. Marine Geology, 97(3–4): 413–421

Bao Gende, Li Quanxing. 1993. Geochemistry of rare earth elements in ferromanganese nodules (crusts) of the South China Sea. Oceanologia et Limnologia Sinica (in Chinese), 24(3): 304–313

Baturin G N, Gorshkov A I, Magazina L O, et al. 2002. Structure and composition of ferromanganese–phosphate nodules from the Black Sea. Lithology and Mineral Resources, 37(4): 374–385

Bau M, Dulski P. 1996. Distribution of yttrium and rare-earth elements in the Penge and Kuruman Fe-formations, Transvaal Supergroup, South Africa. Precambrian Research, 79(1–2): 37–55

Bau M, Koschinsky A. 2009. Oxidative scavenging of Ce on hydrous Fe oxide: evidence from the distribution of rare earth elements and yttrium between Fe oxides and Mn oxides in hydrogenetic ferromanganese crusts. Geochemical Journal, 43(1): 37–47

Bau M, Koschinsky A, Dulski P, et al. 1996. Comparison of the partitioning behaviours of yttrium, rare earth elements, and titanium between hydrogenetic marine ferromanganese crusts and seawater. Geochimica et Cosmochimica Acta, 60(10): 1709–1725

Bau M, Schmidt K, Koschinsky A, et al. 2014. Discriminating between different genetic types of marine ferro-manganese crusts and nodules based on rare earth elements and yttrium. Chemical Geology, 381: 1–9

Bonatti E, Fisher D E, Joensuu O, et al. 1972. Fe-manganese-barium deposit from the northern Afar Rift (Ethiopia). Economic Geology, 67(6): 717–730

Byrne R H, Kim K H. 1990. Rare earth element scavenging in seawater. Geochimica et Cosmochimica Acta, 54(10): 2645–2656

Calvert S E. 1978. Geochemistry of oceanic ferromanganese deposits. Philosophical Transactions of the Royal Society A: Mathematical, Physical and Engineering Sciences, 290(1366): 43–73

Calvert S E, Piper D Z. 1984. Geochemistry of ferromanganese nodules from DOMES site a, Northern equatorial Pacific: multiple diagenetic metal sources in the deep sea. Geochimica et Cosmochimica Acta, 48(10): 1913–1928

Chauhan O S. 2003. Geochemistry of ferromanganese micronodules and associated Mn and trace metals diagenesis at high terrigenous depositional site of middle fan region, Bay of Bengal. Deep-Sea Research : Part II. Topical Studies in Oceanography, 50(5): 961–978

Chen Yuwei, Gui Xuntang. 1998. Isotope Geochemistry of the Nansha Islands Sea Area (in Chinese). Beijing: Science Press, 152–163

Chen Zhong, Yang Huining, Yan Wen, et al. 2006a. Distributions and divisions of mineral resources in the sea areas of China: placer deposit and ferromanganese nodule/crust. Marine Geology & Quaternary Geology (in Chinese), 26(5): 101–108

Chen Shouyu, Zhang Haisheng, Zhao Pendga. 2006b. Rare earth element geochemistry of co-rich crust in the mid-Pacific and South China Sea. Marine Geology & Quaternary Geology (in Chinese), 26(4): 45–50

Chi Ru an, Tian Jun, Luo Xianping, et al. 2012. The basic research on the weathered crust elution-deposited rare earth ores. Nonferrous Metals Science and Engineering (in Chinese), 3(4): 1–13

Conrad T, Hein J R, Paytan A, et al. 2017. Formation of Ferromanganese crusts within a continental margin envFement. Ore Geology Reviews, 87: 25–40

Cui Yingchun, Liu Jihua, Ren Xiangwen, et al. 2009. Geochemistry of rare earth elements in Co-rich crusts from the Mid-Pacific M seamount. Journal of Rare Earths, 27(1): 169–176

Dekov V M, Marchig V, Rajta I, et al. 2003. Ferromanganese micronodules born in the metalliferous sediments of two spreading centres: the East Pacific Rise and Mid-Atlantic Ridge. Marine Geology, 199(1–2): 101–121

Duliu O, Alexe V, Moutte J, et al. 2009. Major and trace element distributions in manganese nodules and micronodules as well as abyssal clay from the Clarion-Clipperton abyssal plain, Northeast Pacific. Geo-Marine Letters, 29(2): 71–83

Dutta T, Kim K H, Uchimiya M, et al. 2016. Global demand for rare earth resources and strategies for green mining. EnvFemental Research, 150: 182–190

Dymond J, Lyle M, Finney B, et al. 1984. Ferromanganese nodules from MANOP Sites H, S, and R-Control of mineralogical and chemical composition by multiple accretionary processes. Geochimica et Cosmochimica Acta, 48(5): 931–949

Ministry of Land and Resources of the People's Republic of China. 2002. DZ/T 0204-2002 Specifications for rare earth minerals exploration. Beijing: Geology Press

German C R, Elderfield H. 1990. Application of the Ce anomaly as a paleoredox indicator: the ground rules. Paleoceanography, 5(5): 823–833

German C R, Holliday B P, Elderfield H. 1991. Redox cycling of rare earth elements in the suboxic zone of the Black Sea. Geochimica et Cosmochimica Acta, 55(12): 3553–3558

Glasby G P, Emelyanov E M, Zhamoida V A, et al. 1997. EnvFements of formation of ferromanganese concretions in the Baltic Sea: a critical review. Geological Society, London, Special Publications, 119(1): 213–237

González F J, Somoza L, Hein J R, et al. 2016. Phosphorites, Co-rich Mn nodules, and Ferromanganese crusts from Galicia Bank, NE Atlantic: reflections of Cenozoic tectonics and paleoceanography. Geochemistry, Geophysics, Geosystems, 17(2): 346–374

González F J, Somoza L, León R, et al. 2012. Ferromanganese nodules and micro-hardgrounds associated with the Cadiz Contourite Channel (NE Atlantic): palaeoenvFemental records of fluid venting and bottom currents. Chemical Geology, 310-311: 56–78

Halbach P, Friedrich G, von Stackelberg U. 1988. The Manganese Nodule Belt of the Pacific Ocean: Geological EnvFement, Nodule Formation, and Mining Aspects. Stuttgart: Ferdinand Enke Verlag, 245

He Liangbiao. 1991. Geochemical characteristics of Ferromanganese nodules and crusts from the Mariana Ridge and the West Philippine Basin. Chinese Science Bulletin, 36(14): 1190–1193

Hein J R, Conrad T A, Frank M, et al. 2012. Copper-nickel-rich, amalgamated ferromanganese crust - nodule deposits from Shatsky Rise, NW Pacific. Geochemistry, Geophysics, Geosystems, 13(10): Q10022

Hein J R, Conrad T A, Staudigel H. 2010. Seamount mineral deposits: a source of rare metals for high-technology industries. Oceanography, 23(1): 184–189

Hein J R, Koschinsky A, Bau M, et al. 2000. Co-rich ferromanganese crusts in the Pacific. In: Cronan D S, ed. Handbook of Marine Mineral Deposits. Boca Raton, FL: CRC Press, 239–279

Hein J R, Koschinsky A, Halbach P, et al. 1997. Fe and manganese oxide mineralization in the Pacific. Geological Society, London, Special Publications, 119(1): 123–138

Hein J R, Koschinsky A, McIntyre B R. 2005. Mercury and silver-rich ferromanganese oxides, southern California borderland: deposit model and envFemental implications. Economic Geology, 100(6): 1151–1168

Hein J R, Koschinsky A, Mikesell M, et al. 2016. Marine phosphorites as potential resources for heavy rare earth elements and yttrium. Minerals, 6(3): 88

Hein J R, Mizell K, Koschinsky A, et al. 2013. Deep-ocean mineral deposits as a source of critical metals for high-and green-technology applications: comparison with land-based resources. Ore Geology Reviews, 51: 1–14

Hein J R, Schwab W C, Davis A. 1988. Co-and platinum-rich ferromanganese crusts and associated substrate rocks from the Marshall Islands. Marine Geology, 78(3–4): 255–283

Hein J R, Spinardi F, Okamoto N, et al. 2015. Critical metals in manganese nodules from the Cook Islands EEZ, abundances and distributions. Ore Geology Reviews, 68(1): 97–116

Huang Mu, Liu Jihua, Shi Xuefa, et al. 2014. Geochemical characteristics and material sources of rare earth elements in sediments from the CC area in the eastern Pacific Ocean. Advances in Marine Science (in Chinese), 32(2): 175–187

Hucrrns J M, Clvrnnon M, Mlnuno A N. 1991. Rare-earth-element ordering and structural variations in natural rare-earth-bearing apatites. American Mineralogist, 76(7–8): 1165–1173

Hughes J M, Rakovan J F. 2015. Structurally robust, chemically diverse: apatite and apatite supergroup minerals. Elements, 11(3): 165–170

Hui Gege, Li Sanzhong, Guo Lingli, et al. 2016. Source and accumulation of gas hydrate in the northern margin of the South China Sea. Marine and Petroleum Geology, 69: 127–145

Kato Y, Fujinaga K, Nakamura K, et al. 2011. Deep-sea mud in the Pacific Ocean as a potential resource for rare-earth elements. Nature Geoscience, 4(8): 535–539

Koschinsky A, Halbach P. 1995. Sequential leaching of marine ferromanganese precipitates: genetic implications. Geochimica et Cosmochimica Acta, 59(24): 5113–5132

Koschinsky A, Halbach P, Hein J R, et al. 1996. Ferromanganese crusts as indicators for paleoceanographic events in the NE Atlantic. Geologische Rundschau, 85(3): 567–576

Koschinsky A, Hein J R. 2003. Uptake of elements from seawater by ferromanganese crusts: solid-phase associations and seawater speciation. Marine Geology, 198(3–4): 331–351

Koschinsky A, Stascheit A, Bau M, et al. 1997. Effects of phosphatization on the geochemical and mineralogical composition of marine ferromanganese crusts. Geochimica et Cosmochimica Acta, 61(19): 4079–4094

Kuhn T, Rühlemann C, Wiedicke-Hombach M. 2012. Developing a strategy for the exploration of vast seafloor areas for prospective manganese nodule fields. In: Zhou H, Morgan C L, eds. Marine Minerals: Finding the Right Balance of Sustainable Development and EnvFemental Protection. Shanghai: The Underwater Mining Institute, 1–9

Kynicky J, Smith M P, Xu Cheng. 2012. Diversity of rare earth deposits: the key example of China. Elements, 8(5): 361–367

Liang Hongfeng, Yao De, Liang Dehua. 1991. Geochemistry of polymetelallic crust from JianFeng Seamount, South China Sea. Marine Geology & Quaternary Geology (in Chinese), 11(4): 49–57

Lin Zhenhong, Ji Fuwu, Zhang Fuyuan, et al. 2003. Characteristics and origin of ferromanganese nodules from the northeastern continental slope of the South China Sea. Marine Geology & Quaternary Geology (in Chinese), 23(1): 7–12

Liu Jianguo, Chen Zhong, Yan Wen, et al. 2010. Geochemical characteristics of rare earth elements in the fine-grained fraction of surface sediment from South China Sea. Earth Science-Journal of China University of Geosciences (in Chinese), 35(4): 563–571

Liu Zhifei, Colin C, Li Xiajing, et al. 2010. Clay mineral distribution in surface sediments of the northeastern South China Sea and surrounding fluvial drainage basins: source and transport. Marine Geology, 277(1–4): 48–60

Long K R, Van Gosen B S, Foley N K, et al. 2012. The principal rare earth elements deposits of the United States: a summary of domestic deposits and a global perspective. In: Sinding-Larsen R, Wellmer F W, eds. Non-Renewable Resource Issues. Dordrecht: Springer, 131–155

Marino E, González F J, Somoza L, et al. 2017. Strategic and rare elements in Cretaceous-Cenozoic Co-rich ferromanganese crusts from seamounts in the Canary Island Seamount Province (northeastern tropical Atlantic). Ore Geology Reviews, 87: 41–61

Milliman J D, Farnsworth K L. 2011. River Discharge to the Coastal Ocean: A Global Synthesis. New York: Cambridge University Press

Moffett J W. 1990. Microbially mediated Ce oxidation in sea water. 345(6274): 421–423.

Mills R A, Wells D M, Roberts S. 2001. Genesis of ferromanganese crusts from the TAG hydrothermal field. Chemical Geology, 176(1–4): 283–293

Muinos S B, Hein J R, Frank M, et al. 2013. Deep-sea Ferromanganese crusts from the northeast Atlantic Ocean: composition and resource considerations. Marine Georesources & Geotechnology, 31(1): 40–70

Mukhopadhyay R, Iyer S D, Ghosh A K. 2003. The Indian Ocean nodule field: petrotectonic evolution and ferromanganese deposits. Earth-Science Reviews, 60(1–2): 67–130

Ohta A, Ishii S, Sakakibara M, et al. 1999. Systematic correlation of the Ce anomaly with the Co/(Ni+Cu) ratio and Y fractionation from Ho in distinct types of Pacific deep-sea nodules. Geochemical Journal, 33(6): 399–417

Orris G J, Grauch R I. 2002. Rare earth element mines, deposits, and occurrences. Open-File Report 2002–189. Washington DC: U.S. Geological Survey

Papavasileiou K. 2014. Near future REE resources for Europe-the new frontier of marine exploration, mining and processing. In: ERES 2014: 1st European Rare Earth Resources Conference. Milos Island, Greece: ERES, 410–427

Pattan J N, Parthiban G. 2011. Geochemistry of ferromanganese nodule–sediment pairs from Central Indian Ocean Basin. Journal of Asian Earth Sciences, 40(2): 569–580

Piper D Z. 1974. Rare earth elements in ferromanganese nodules and other marine phases. Geochimica et Cosmochimica Acta, 38(7): 1007–1022

Pourret O, Davranche M. 2013. Rare earth element sorption onto hydrous manganese oxide: a modeling study. Journal of Colloid and Interface Science, 395: 18–23

Prakash L S, Ray D, Paropkari A L, et al. 2012. Distribution of REEs and yttrium among major geochemical phases of marine Ferromanganese-oxides: comparative study between hydrogenous and hydrothermal deposits. Chemical Geology, 312-313: 127–137

Qu Tangdong, Du Yan, Sasaki H. 2006. South China Sea throughflow: a heat and freshwater conveyor. Geophysical Research Letters, 332(23): L23617

Rajani R P, Banakar V K, Parthiban G, et al. 2005. Compositional variation and genesis of ferromanganese crusts of the Afanasiy-Nikitin Seamount, equatorial Indian Ocean. Journal of Earth System Science, 114(1): 51–61

Reyss J L, Marchig V, Ku T L. 1982. Rapid growth of a deep-sea manganese nodule. Nature, 295(5848): 401–403

Rona P A. 2008. The changing vision of marine minerals. Ore Geology Reviews, 33(3–4): 618–666

Schulz H D. 2006. Quantification of early diagenesis: dissolved constituents in pore water and signals in the solid phase. In: Schulz H D, Zabel M, eds. Marine Geochemistry. Berlin Heidelberg: Springer, 73–124

Sholkovitz E R, Landing W M, Lewis B L. 1994. Ocean particle chemistry: the fractionation of rare earth elements between suspended particles and seawater. Geochimica et Cosmochimica Acta, 58(6): 1567–1579

Stoffers P, Glasby G P, Frenzel G. 1984. Comparison of the characteristics of manganese micronodules from the equatorial and South-West Pacific. Tschermaks Mineralogische und Petro-

graphische Mitteilungen, 33(1): 1–23
Su W. 2009. Economic and policy analysis of China's rare earth industry (in Chinese). Beijing: China Financial and Economic Publishing House
Takahashi Y, Manceau A, Geoffroy N, et al. 2007. Chemical and structural control of the partitioning of Co, Ce, and Pb in marine ferromanganese oxides. Geochimica et Cosmochimica Acta, 71(4): 984–1008
Van Gosen B S, Verplanck P L, Long K R, et al. 2014. The rare-earth elements: vital to modern technologies and lifestyles. Fact Sheet 2014-3078. Reston, VA: U.S. Geological Survey
Wang Xianjue, Chen Yuwei, Wu Mingqing. 1984. Geochemistry of re and trace elements in ferromanganese nodules and their genesis. Chinese Journal of Oceanology and Limnology, 4(3): 211–226
Wang Pinxian, Li Qianyu. 2009. History of the South China Sea-A synthesis. In: Wang Pinxian, Li Qianyu, eds. The South China Sea: Paleoceanography and Sedimentology. Dordrecht: Springer, 487–496
Wegorzewski A V, Kuhn T. 2014. The influence of suboxic diagenesis on the formation of manganese nodules in the Clarion Clipperton nodule belt of the Pacific Ocean. Marine Geology, 357: 123–138
Weng Zhehan, Jowitt S M, Mudd G M, et al. 2015. A detailed assessment of global rare earth element resources: opportunities and challenges. Economic Geology, 110(8): 1925–1952
Xu Zhaokai, Li Anchun, Jiang Fuqing, et al. 2006. Characteristics and origin of the new-type ferromanganese crusts from deepwater areas of the East Philippine Sea. Marine Geology & Quaternary Geology (in Chinese), 26(4): 91–98
Yao Bo chu, Zeng Weijun, Hayer D E, et al. 1994. The Geological Memoir of South China Sea Surveyed jointly by China and the U.S.A. (in Chinese). Wuhan: The Press of Chinese Gological University
Zhang Zhenguo, Du Yuansheng, Gao Lianfeng, et al. 2012. Enrichment of REEs in polymetallic nodules and crusts and its potential for exploitation. Journal of Rare Earths, 30(6): 621–626
Zhang Zhenguo, Du Yuansheng, Wu Changhang, et al. 2013. Growth of a polymetallic nodule from northwestern continental margin of the South China Sea and its response to changes in paleoceanographical envFement of the Late Cenozoic. Science China: Earth Sciences, 56(3): 453–463
Zhang Dechao, Liu Yanxia, Li Xinzheng. 2015. Characterization of bacterial diversity associated with deep sea ferromanganese nodules from the South China Sea. Journal of Microbiology, 53(9): 598–605
Zhong Yi, Chen Zhong, González F J, et al. 2017a. Composition and genesis of ferromanganese deposits from the northern South China Sea. Journal of Asian Earth Sciences, 138: 110–128
Zhong Yi, Chen Zhong, Mo Aibin, et al. 2017b. Genetic types and elemental occurrence phases of ferromanganese nodules in the northern South China Sea. Journal of Tropic Oceanology (in Chinese), 36(2): 48–59